Effect of Noncovalent Interactions on Vibronic Transitions: An Experimental and Theoretical Study of the C2H...CO2 Complex

Effect of noncovalent interactions on vibronic transitions: An experimental and theoretical study of the $C_2H\cdots CO_2$ complex

Sergey V. Ryazantsev,[a],[b] Riccardo Tarroni,[c] Vladimir I. Feldman,[b] and Leonid Khriachtchev*[a]

We report on the experimental and theoretical infrared spectrum of the $C_2H\cdots CO_2$ complex. This complex was prepared by UV photochemistry of propiolic acid (HC_3OOH) in argon and krypton matrices. The experimental bands of C_2H in the $C_2H\cdots CO_2$ complex are blue-shifted from those of C_2H monomer. The calculations of the $C_2H\cdots CO_2$ structures were performed at the RMP2/aug-cc-pVTZ level. The relative stability of the complex structures was evaluated using the RCCSD(T)/aug-cc-pVQZ level. In order to simulate the spectrum of the $C_2H\cdots CO_2$ complex, we developed the theoretical approach used earlier for C_2H monomer. Based on the calculations, the main experimental bands of the $C_2H\cdots CO_2$ complex are assigned to the most stable parallel structure. Practically all strong bands predicted by theory (>30 km mol^{-1}) are observed in the experiment. To our knowledge, it is the first study of the effect of noncovalent interaction on vibronic transitions and the first report on an intermolecular complex of C_2H radical.

[a] S. V. Ryazantsev, Dr. L. Khriachtchev
Department of Chemistry, University of Helsinki, P. O. Box 55, FI-00014 Helsinki, Finland
E-mail: leonid.khriachtchev@helsinki.fi

[b] S. V. Ryazantsev, Prof. V. I. Feldman
Department of Chemistry, Lomonosov Moscow State University, Moscow 119991 Russia

[c] Prof. R. Tarroni
Dipartimento di Chimica Industriale "Toso Montanari", Università di Bologna, Viale Risorgimento 4, 40136 Bologna, Italy

Supporting information for this article is given via a link at the end of the document.

Introduction

Noncovalent interactions are crucial for understanding numerous properties of matter and have been an important area of research for many years. [1–11] These interactions (with stabilization energies of ~4–80 kJ mol^{-1}) play significant roles in many fields of physics, chemistry, and biology, for example, in atmospheric and combustion chemistry and in catalysis. The properties of molecules in complexes change compared to the monomers. In particular, the optical spectra of interacting molecules differ from those of the monomers. The complexation-induced changes can be also simulated theoretically, allowing structural assignment based on the experimental results. Many kinds of intermolecular complexes have been studied, and the majority of those studies deal with closed-shell species and the ground electronic state. Indeed, open-shell species and excited electronic states are much more difficult for both experiment and theory.

The main goal of the present work is to explore the effect of noncovalent interactions on vibronic transitions that involve a simultaneous change in the electronic and vibrational states of the system.[12,13] Ethynyl radical (C_2H) is a particularly good candidate for this study. The specific electronic structure of C_2H results in the appearance of a rich spectrum in the infrared region.[14,15] This species plays important roles in combustion and astrochemistry;[16–19] thus, its intermolecular interactions are of a clear interest. C_2H radical has been extensively characterized by electronic, vibrational, and EPR spectroscopies;[14,20–26] however, intermolecular complexes of this species are unknown.

The theoretical understanding of the infrared spectrum even of C_2H *monomer* is a non-trivial task, which cannot be handled using the commercial quantum chemical programs. The routine methods to calculate vibrational spectra rely on the Born-Oppenheimer approximation, i.e. a strict separation of the electronic and nuclear motions. This approximation is valid for the ground state of most molecular species because the energy of the first excited electronic state is usually much larger than the vibrational energies. However, it is not the case for C_2H radical because the first electronic transition and the CH stretching mode appear at similar energies,[15] which is quite unique for neutral radicals. The problem is even more complex because the first excited electronic state of C_2H has Π symmetry, thus, experiencing inter-electronic couplings due to the Renner-Teller effect.[27] It follows that the infrared absorption spectrum of C_2H can be treated quantitatively only employing a variational approach and considering explicitly the three-state vibronic coupling.[28] In this way, Tarroni and Carter calculated the vibronic transitions[15] and the absorption intensities[29] of C_2H. The high accuracy of those calculations has been confirmed by the recent experiments on C_2H in the gas phase,[30,31] with differences less than 10 cm^{-1} for frequencies up to 7100 cm^{-1}. Vibronic coupling also takes place for C_2X radicals (X = F, Cl, Br).[32–37]

Among different experimental methods, matrix-isolation infrared spectroscopy is a powerful tool to study noncovalent interaction.[38–40] This technique can be successfully applied to complexes of free radicals that are often difficult to study by other experimental methods because of their high reactivity. The low temperature allows one to measure the

spectrum over extended periods of time without essential perturbation from the surrounding. One of the practical ways to prepare intermolecular complexes includes in-situ UV photolysis of molecules embedded in inert matrices.[40] This method produces complexes with a higher concentration than it can be achieved by co-deposition of two molecular species. For example, photolysis of propiolic acid (PA, HC_3OOH) in noble-gas matrices mainly leads to the $C_2H_2\cdots CO_2$ complex.[41] Intuitively, further photolysis of the $C_2H_2\cdots CO_2$ complex can produce the $C_2H\cdots CO_2$ complex because photolysis of matrix-isolated C_2H_2 leads to C_2H monomers.[42,43] Tanskanen *et al.* seemed to report an indirect evidence of this process.[44] They photolyzed PA in a xenon matrix and observed the annealing-induced formation of the $HXeCCH\cdots CO_2$ complex, whose precursor was presumably the $C_2H\cdots CO_2$ complex. However, the experimental identification of this elusive radical-molecule complex is missing. The $C_2H\cdots CO_2$ complex is an excellent model system for exploring the effect of noncovalent interactions on vibronic transitions. It has been shown that photolysis of matrix-isolated acyl peroxides produces radical pairs separated by two molecules of CO_2.[45–48]

In the present work, we report on the experimental and theoretical infrared spectrum of the $C_2H\cdots CO_2$ complex. This complex is obtained by UV photochemistry of PA in argon and krypton matrices. The assignment is based on the good agreement between the experimental and theoretical spectra. In order to simulate the effect of noncovalent interactions on the vibronic transitions of C_2H radical, we develop the theoretical approach used previously for C_2H monomer.[15,29] To our knowledge, it is the first study of the effect of noncovalent interaction on vibronic transitions and the first report on an intermolecular complex of C_2H radical.

Calculations

Structures of the $C_2H\cdots CO_2$ complex

The calculations were performed with the Molpro suite of quantum chemical programs (version 2010.1)[49] at the restricted second order Møller-Plesset (RMP2)[50,51] level of theory with the aug-cc-pVTZ basis set.[52,53] The convergence criteria for the optimization process were the Molpro default, i.e. the maximum component of the energy gradient was less than 3×10^{-4} a.u. and the maximum energy change was less than 10^{-6} hartree. However, the numerical energy gradients were calculated using a more accurate four-point formula, instead of the default two-point scheme. The harmonic vibrational frequencies were finally calculated at the same level of theory. The interaction energies were calculated as the differences between the energies of the complexes and the monomers using the larger aug-cc-pVQZ basis set,[52,53] both at the RMP2 level and at the restricted coupled-cluster singles and doubles[54] with perturbative triples corrections (RCCSD(T)).[55] The energies were corrected for the basis set superposition error (BSSE)[56] and for the zero-point vibrational energy (ZPVE).

Table 1. Calculated structural parameters (r in Å; θ and τ in degrees), interaction energies (in cm^{-1}), and harmonic vibrational frequencies (in cm^{-1}) of the $C_2H\cdots CO_2$ complex structures. [a]

	Mon.	Paral.	Lin. (1)	Lin. (2)	Perpen.
		Structural parameters [b]			
$r_{(H1-C1)}$	1.0621	1.0627	1.0633	1.0621	1.0623
$r_{(C1-C2)}$	1.2151	1.2159	1.2155	1.2155	1.2151
$r_{(C3-O1)}$	1.1702	1.1705	1.1712	1.1706	1.1704
$r_{(C3-O2)}$	1.1702	1.1696	1.1683	1.1698	1.1704
$r_{(C1-C3)}$		3.2175			
$r_{(H1-O1)}$			2.3015		
$r_{(C2-O1)}$				3.0822	
$r_{(C2-C3)}$					3.3183
$\theta_{(H1-C1-C2)}$	180.00	179.26	180.00	179.99	180.00
$\theta_{(O1-C3-O2)}$	180.00	179.56	180.00	180.00	179.86
$\theta_{(C1-H1-O1)}$			180.00		
$\theta_{(C1-C2-O1)}$				179.77	
$\theta_{(C1-C2-C3)}$					180.00
$\theta_{(O1-C3-C1)}$		79.01			
$\theta_{(C2-C1-C3)}$		80.90			
$\tau_{(C3-C2-C1-H1)}$		29.74			
$\tau_{(O1-C3-C1-C2)}$		179.85			
$\tau_{(O2-C3-C1-H1)}$		179.48			
$\tau_{(C1-C2-O1-C3)}$				173.70	
		Interaction energies [c]			
E_{int} (RMP2)		–745	–537	–239	–145
E_{int} (RCCSD(T))		–653	–529	–222	–98
E_{int} (RCCSD(T)/ BSSE)[d]		–621	–458	–181	–67
E_{int} (RCCSD(T)/ BSSE/ ZPVE)[e]		–458	–169	+11	+172
		Harmonic vibrational frequencies [f]			
CH stretch	3482.5	3475.5	3480.9	3483.5	3488.4
CC stretch	1984.8	1980.4	1982.6	1983.3	1987.3
CCH bend	344.8	366.7	417.3	397.1	370.3
	344.8	368.6	417.3	412.2	375.5
a-CO stretch	2400.7	2401.3	2406.4	2401.4	2399.2
s-CO stretch	1325.7	1327.2	1330.5	1326.8	1327.0
OCO bend	658.8	649.8	659.2	661.3	661.8
	658.8	658.7	659.2	661.4	663.1
Intermol. modes		54.4	52.8	45.2	51.3
		62.3	52.8	57.5	102.4
		84.6	97.8	76.7	130.1
		90.9	110.7	81.4	130.1
			110.7		

[a] Equilibrium structures and labeling of the atoms are shown in Fig. 1. [b] Calculated at the RMP2/aug-cc-pVTZ level of theory. [c] Calculated with the aug-cc-pVQZ basis at the RMP2/aug-cc-pVTZ equilibrium geometries. [d] BSSE corrected value. [e] BSSE and ZPVE corrected value. The harmonic frequencies reported in this table have been used to calculate the ZPVE. [f] Calculated from the energy hessian, neglecting anharmonic and vibronic effects.

Four potentially stable structures were found for the $C_2H\cdots CO_2$ complex (Fig. 1). Their geometries, interaction energies, and harmonic frequencies are shown in Table 1. The two most stable structures, parallel and linear (1), are comparable to the structures of the corresponding $C_2H_2\cdots CO_2$ complex.[41,57,58] In fact, the intermolecular distances in these two cases are very similar, with the differences below 4%. However, the so-called “parallel” structure in the present case is not completely parallel and planar. This lack of symmetry makes the search of the equilibrium structural parameters and the calculation of the harmonic frequencies very lengthy because the calculations should be performed in C_1 symmetry. This requirement prevents the use of a higher level of theory for the

determination of the equilibrium structures. The interaction is about three times stronger in the parallel that in linear (1) structure. The linear (2) and perpendicular structures have positive interaction energies after ZPVE and BSSE corrections and are not considered further.

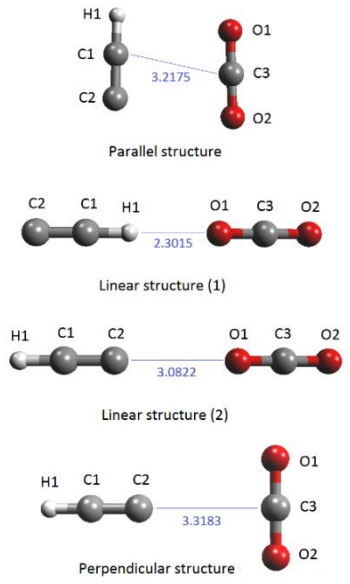

Figure 1. Calculated structures of the $C_2H\cdots CO_2$ complex. The intermolecular distance (in Å) is shown. The other structural parameters are reported in Table A. The parallel structure and the linear structure (2) are slightly non-planar with C_1 symmetry. The linear structure (1) has $C_{\infty v}$ symmetry, while the perpendicular structure has C_{2v} symmetry.

It should be noted that the vibrational frequencies of C_2H calculated at the RMP2 level differ considerably from the gas-phase experimental values[59] and from the best available calculations.[15] This difference is mainly due to the intrinsic limitations of the RMP2 method[60] and to the neglected anharmonicity and the vibronic coupling effects taking place even for the lowest vibrational levels. For this reason, these vibrational frequencies of C_2H cannot be used either to assist the assignment of the experimental spectrum or to make the structural assignment of the $C_2H\cdots CO_2$ complex. We calculated the vibrational spectra at this level mainly to justify (due to the absence of imaginary frequencies) that the found structures are true minima on the potential energy surface (PES) and to estimate the ZPVE correction, i.e. the difference between the ZPVE of the monomers and the complexes. The ZPVE correction is expected to be scarcely affected by the anharmonicity and vibronic effects, since these effects are similar in the monomers and the complexes. In addition, the frequencies of CO_2 in the complex are probably more reliable because for CO_2, the vibronic effects in the ground state are negligible and the anharmonicity is relatively small.

Vibronic spectrum of the $C_2H\cdots CO_2$ complex

The trial computations on the two most stable $C_2H\cdots CO_2$ structures (parallel and linear (1)) have shown that it is impossible to follow exactly the same approach used previously for C_2H monomer,[15,29] even for the linear (1) structure. The reasons are mainly two. First, the approach developed in Ref. [28] and then applied to C_2H[15,29] is specific for three-atom systems. Second, the number of valence electrons to be correlated in the electronic structure calculations of the $C_2H\cdots CO_2$ complex is too large, which would force us to use a lower level of theory and decrease the accuracy of the results. With the available computational tools, it is impossible to calculate the full PES of the complex with a similar accuracy to that of C_2H monomer. In the calculations of C_2H monomer, the internally contracted multireference configuration interaction (ICMRCI) method[61] and the cc-pV5Z basis[52,53] were used and core correlation effects were taken into account. Nevertheless, the calculated Σ^+–Π energy separation was still about 80 cm^{-1} too small and it was empirically set to be 3624 cm^{-1} in order to reproduce the observed infrared gas-phase band origins.[15]

To model the $C_2H\cdots CO_2$ interaction, we modified the $X^2\Sigma^+$ and $A^2\Pi$ PESs of C_2H monomer, whereas the dipole moment surfaces remained unchanged. In practice, we assumed that the interaction with CO_2 significantly affects only the Σ^+–Π energy separation. This assumption is quite strong; however, it is justified by the experimental results described below.

To make a fully *ab initio* estimate of the complexation effect on the Σ^+–Π energy separation of C_2H, we performed a series of the CCSD(T)/aug-cc-pVTZ calculations for the two most stable $C_2H\cdots CO_2$ structures (parallel and linear (1)). Coupled-cluster methods are known to converge to the lowest eigenvalue of a certain symmetry, thus, they can be used to calculate only those excited states that have a single determinant character and a different symmetry than the ground state.[62] This condition is met for the linear (1) structure since it has C_∞ symmetry and the ground and the first excited states have Σ^+ and Π symmetries, respectively. In contrast, the equilibrium structure of the parallel complex has C_1 symmetry, hence all electronic states belong to the same group representation. In order to use CCSD(T) also for the parallel structure, we first slightly modified it in order to obtain a planar geometry. This was achieved by setting the $\tau_{(C3\text{-}C2\text{-}C1\text{-}H1)}$ dihedral angle to 0° and the $\tau_{(O1\text{-}C3\text{-}C1\text{-}C2)}$ and $\tau_{(O2\text{-}C3\text{-}C1\text{-}H1)}$ dihedral angles to 180°. The resulting structure has an energy only 0.2 cm^{-1} higher than the fully optimized one. This "planarization" of the parallel structure was mandatory, in order to have a complex with C_s symmetry. In this point group, the ground state (corresponding to the $X^2\Sigma^+$ state of C_2H monomer) has A′ symmetry whereas the first excited state (corresponding to one component of the degenerate $A^2\Pi$ state of C_2H monomer) has A″ symmetry. In the C_s point group, the other component of the $A^2\Pi$ state of C_2H has A´ symmetry, the same as the ground state, hence it cannot be calculated using CCSD(T). Thus, we have to assume that the complexation affects both components of the Π state similarly, i.e. the degeneracy of the $A^2\Pi$ state is not removed by complexation.

The CCSD(T)/aug-cc-pVTZ calculations were performed at a grid of 49 points around the equilibrium geometries of the two complex structures. The grid was generated by varying the CC bond length from 2.1 to 2.7 bohr in steps of 0.1 bohr and the CH bond length from 1.7 to 2.3 bohr in steps of 0.1 bohr. The equilibrium energies of the ground and excited states of both structures were found

by fitting the energies of the grid with a two-dimensional fourth-degree polynomial.

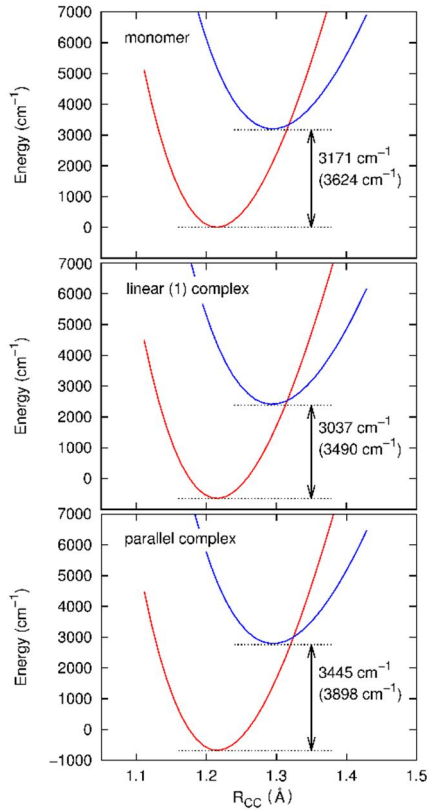

Figure 2. One-dimensional plots along the R_{CC} stretching coordinate of the PES of C_2H calculated at the CCSD(T)/aug-cc-pVTZ level for the monomer and the linear (1) and parallel complexes. The remaining geometrical parameters are set to the values presented in Table I, except the torsional parameters of the parallel complex, whose values are set either to 0º or to 180º (see text for details). The red and blue lines represent the ground $X^2\Sigma^+$ state and the first excited $A^2\Pi$ state of C_2H monomer or the corresponding electronic states of the complexes. The calculated Σ^+–Π separation is also shown, with the corrected value used in the spectrum calculation in parentheses.

In order to obtain *the changes* of the Σ^+–Π energy separation upon complexation, we also simulated the dissociated complex. The calculations of C_2H monomer were performed at the CCSD(T)/aug-cc-pVTZ level at the same 49-point grid of the CC and CH bond lengths and with a bending angle of 180º. The obtained energies were added to the (constant) energy of CO_2 calculated at the same level of theory. As previously, the equilibrium energies of the ground and excited states of the reference (dissociated) system have been determined by fitting the energies of the grid with a two-dimensional fourth-degree polynomial. From these calculations, we obtained the following values for the Σ^+–Π energy separation: 3171 cm^{-1} for C_2H monomer, 3037 cm^{-1} for the linear (1) structure (change of –134 cm^{-1}) and 3445 cm^{-1} for the parallel structure (change of +274 cm^{-1}). In Fig. 2, we show the plots of the two lowest electronic states of C_2H along the CC stretching coordinate for the monomer, the linear (1) structure, and the parallel structure. It is seen that the energies of both the $^2\Sigma^+$ and $^2\Pi$ states decrease upon complexation (as it should be for stable complexes). However, in the linear (1) structure, the $^2\Pi$ state is lowered *more* than the $^2\Sigma^+$ state, thus *reducing* the Σ^+–Π separation. In contrast, in the parallel structure, the $^2\Pi$ state is lowered *less* than the $^2\Sigma^+$ state, hence the Σ^+–Π energy separation increases.

At the CCSD(T)/aug-cc-pVTZ level of theory, the calculated Σ^+–Π energy separation of C_2H monomer is about 450 cm^{-1} lower than the optimal value of 3624 cm^{-1} found previously,[15] showing the extreme difficulty of achieving the so called "spectroscopic accuracy" (i.e. accuracy of 1 cm^{-1} or better) whenever electronic excitations are involved. However, in the present work, we are interested only in the changes of the energy separation upon complexation, whose accuracy is expected to be better due to the error cancellation. These changes, added to the optimal value of 0.016510 hartree (3624 cm^{-1}), give the new $C_{000}^{\Pi+}$ and $C_{000}^{\Pi-}$ coefficients used to calculate the spectrum.[15] These new values are 0.01590 hartree (3490 cm^{-1}) for the linear (1) structure and 0.01776 hartree (3898 cm^{-1}) for the parallel structure (see also Figure 2).

Finally, variational calculations were performed with the RVIB3 code[28] and the same input used previously for the monomer.[15] The selected results of the calculations on the linear (1) and parallel structures are shown in Table 2 where they are compared with the experimental results (described below). From this comparison, it is clear that only the parallel structure is able to reproduce the blue shifts of vibronic transitions observed experimentally. Table 3 shows all transitions with substantial intensities in the experimental spectral region calculated for the parallel structure.

Table 2. Selected experimental frequencies of C_2H in the $C_2H\cdots CO_2$ complex in argon and krypton matrices and calculated vibronic transitions for the linear (1) and parallel structures (in cm^{-1}).[a]

Exp. (Ar)	Exp. (Kr)	Linear (1)	Parallel
1839.7 (–6.9)	1852.3	1830.9 (–7.1)	1851.2 (+13.2)
1856.8 (+10.2)	(+10.3)		
4181 (+46)	4148 (+36)	4072.8 (–20.8)	4209.4 (+115.8)
4278 (+143)	4247 (+135)		
5358 (+17)	5335 (+19)	5313.0 (–15.8)	5362.9 (+34.1)
5522 (+49)	5487 (+35)	5411.4 (–33.5)	5517.9 (+73.0)
5648 (+74)	5606 (+57)	5494.0 (–32.2)	5649.1 (+121.9)
5708 (+56)	5670 (+40)	5586.2 (–43.6)	5705.0 (+75.2)
5740 (+88)	*5733 (+103)*		
5968 (+58)	5933 (+44)	5860.1 (–22.1)	5942.7 (+60.5)

[a] Complexation-induced shifts are shown in parentheses; tentative assignments are *in italics*.

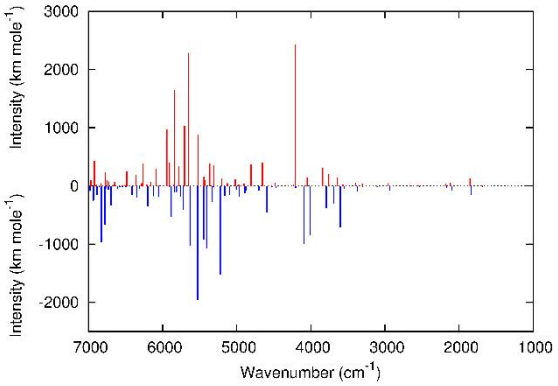

Figure 3. Simulated absorption spectra of the C_2H monomer (blue/negative) and of the parallel structure of the $C_2H\cdots CO_2$ complex (red/positive) at the temperature of 5 K. Each stick represents the sum of the intensities of all rotational transitions (up to J = 7/2) originating from the same vibronic band, each centered at the energy of the lowest rotational transition.

Table 3. Calculated (parallel structure) and experimental (argon matrix) vibronic spectrum of C_2H monomer and of C_2H in the $C_2H\cdots CO_2$ complex (frequencies in cm^{-1}). [a]

Calculations			Argon matrix		
Monomer [b]	Parallel structure	Shift	Monomer	Complex	Shift [c]
1232.3 (4.3)	1238.5 (3.3)	+6.2	1240.4	–	–
1682.0 (16.6)	1688.8 (11.2)	+6.8	1686.1	–	–
1838.0 (146.1)	1851.2 (124.3)	+13.2	1846.6	*1839.7*	*–6.9*
				1856.8	+10.2
				1862.6 sh	+16.0
2096.8 (73.5)	2117.8 (50.5)	+21.0	2105	*2124*	*+19*
2166.8 (34.1)	2176.2 (36.1)	+9.4	2175	–	–
2536.1 (13.2)	2551.4 (11.9)	+15.3	2545	–	–
2640.4 (9.0)	2645.5 (7.8)	+5.1	2648	–	–
2933.7 (81.0)	2957.5 (48.6)	+23.8	2944	2975	+31
3371.1 (86.5)	3393.9 (55.5)	+22.8	3381	3399	+18
3546.9 (46.1)	3567.4 (28.5)	+20.5	3555	–	–
3604.4 (6.9)	3642.8 (152.7)	+38.4	–	3627	[d]
				3656	
3604.6 (702.7)	3621.7 (16.6)	+17.1	3609	–	–
			3614		
3690.5 (301.6)	3758.1 (212.4)	+67.6	3731	3810	+79
3790.9 (374.0)	3839.5 (309.1)	+48.6	3806	3841	+35
4011.4 (845.4)	4047.8 (154.1)	+36.4	4022	4069	+47
				4090	*+68*
4093.6 (977.3)	4209.4 (2426.4)	+115.8	4112 sh	4181	+46
			4135	4278	+143
4204.1 (37.5)	4234.9 (21.4)	+30.8	4224	–	–
4470.4 (38.2)	4481.2 (53.5)	+10.8	4478	4513	+35
4524.1 (15.9)	4528.8 (8.4)	+4.7	4522	–	–
4592.7 (459.0)	4652.6 (398.8)	+59.9	4622	4666	+44
				4710	+88
				4730 sh	*+108*
4701.5 (77.1)	4807.8 (366.6)	+106.3	*4731*	*4799*	*+68*
				4821	*+90*
				4874	*+143*
4886.9 (118.9)	4902.0 (37.5)	+15.1	4894	*4900*	*+6*
				4925	*+31*
4966.7 (171.2)	5018.6 (112.2)	+51.9	4999	5048	+49
5004.8 (64.0)	5066.6 (0.4)	+61.8	–	–	–
5094.8 (153.9)	5123.9 (46.9)	+29.1	5112	–	–
5160.8 (157.9)	5199.5 (124.7)	+38.7	5178	*5230*	*+52*
5221.9 (1518.3)	5311.7 (349.8)	+89.8	5235	5270	+35
			5241	5307	+72
5328.8 (277.0)	5362.9 (381.3)	+34.1	5341	5358	+17
5405.7 (1065.9)	5442.2 (164.1)	+36.5	5416	5468	+52
5444.9 (914.6)	5517.9 (877.9)	+73.0	5473	5522	+49
5527.2 (1956.3)	5649.1 (2287.5)	+121.9	5557	*5591*	*+17*
			5574	*5606*	*+32*
				5648	+74
5629.8 (1233.2)	5705.0 (1030.8)	+75.2	5652	5708	+56
				5740	+88
				5772	*+120*
5720.6 (403.2)	6045.6 (6.6)	+325.0	5765	–	–
5757.0 (181.1)	5778.6 (339.0)	+21.6	~ 5787 [e]	*5841*	*+54*
5812.9 (101.9)	5841.1 (1646.5)	+28.2	--	*5913*	[d]
5837.6 (104.2)	5851.2 (31.1)	+13.6	5852	–	–
5882.2 (534.6)	5942.7 (968.4)	+60.5	5910	5968	+58
6054.1 (186.9)	6086.0 (288.0)	+31.9	6078	6137	+59
6120.8 (175.2)	6160.8 (75.1)	+40.0	6142	*6168*	*+26*
6200.7 (19.6)	6264.7 (390.8)	+64.0	--	*6288*	[d]
6201.3 (349.5)	6211.2 (29.1)	+9.9	6236	-	-

[a] Calculated intensities (in km mol^{-1}) are given in parentheses; tentative assignments are *in italics*; sh – shoulder. [b] From Refs. [15] and [29]. [c] When the monomer absorption is structured, the complexation-induced shift is calculated with respect to the most intense component. [d] Experimental shift could not be extracted since the corresponding absorption of the monomer is not detected. [e] Very broad and hardly visible.

For the parallel and linear (1) structures, the intensities were also calculated, using the dipole moment surfaces of the isolated C_2H.[29] It means that the effects of the complexation on the intensities are accounted for only through the changes of the vibronic wavefunctions. The calculated intensities of C_2H monomer and of the parallel structure are presented in Table 3 and Fig. 3. Below 3500 cm^{-1}, all intensities of the complex are similar to those of C_2H monomer. Above 3500 cm^{-1}, there are substantial changes in the intensities of some transitions. For example, the complex band at 4209.4 cm^{-1} of the parallel structure (corresponding to the 4093.6 cm^{-1} band of the monomer) substantially increases in intensity and becomes the most prominent in the spectrum, whereas the bands at 4047.8, 5311.7, and 5442.2 cm^{-1} (corresponding to the bands of the monomer at 4011.4, 5221.9 and 5405.7 cm^{-1}, respectively) substantially decrease in intensity. Table S1 (Supporting Information) shows all calculated frequencies, intensities, and complexation-induced shifts for C_2H monomer and for the linear (1) and parallel structures of the complex.

Experimental results

C_2H monomers in argon and krypton matrices were obtained by 193-nm photolysis of C_2H_2/Ar and C_2H_2/Kr matrices. The CC stretching band of C_2H monomer is observed at 1846.6 and 1842.0 cm^{-1} in argon and krypton matrices, respectively.[14,26,43] In addition, a large number of vibronic bands appear at higher frequencies, in reasonable agreement with the literature data.[14,26] The vibronic bands of C_2H in a krypton matrix are red-shifted typically by 20–30 cm^{-1} from those in an argon matrix (see Table 3 and Table S2 in Supporting Information) but their relative positions and intensities remain similar.

In attempts to prepare the $C_2H\cdots CO_2$ complexes, PA/Ng (Ng = Ar and Kr) matrices were first irradiated at 193 nm. 193-nm photolysis of matrix-isolated PA has been studied previously and the $C_2H_2\cdots CO_2$ complex (parallel structure) is the main primary product.[41] In addition, the $HC_2OH\cdots CO$ and $C_3O\cdots H_2O$ complexes were suggested to be minor primary photoproducts. Ketenyl radical (HC_2O)[14] and some other species are also formed in small amounts as previously mentioned in Ref. [41] (presumably via secondary photoreactions). HC_2O is presumably complexed with CO because it is believed to originate from the $HC_2OH\cdots CO$ and/or $H_2C_2O\cdots CO$ complexes. However, the direct spectroscopic evidence of this complex is difficult to obtain because the complexation-induced effect on HC_2O is very small and the CO stretching region is very crowded by other products of PA photolysis.

Spectrum a in Fig. 4 shows the formation of the $C_2H_2\cdots CO_2$ and $HC_2O\cdots CO$ (2019.1/2023.8 cm^{-1}) complexes as a result of 193-nm photolysis of PA in an argon matrix. In addition, bands suitable for the $C_2H\cdots CO_2$ complex are observed, particularly, a characteristic band at 1856.8 cm^{-1} (blue-shifted from the band of C_2H monomer by +10.2 cm^{-1}) as well as the characteristic series of vibronic bands at higher frequencies, similarly to the case of C_2H monomer. The $C_2H\cdots CO_2$ bands saturate relatively quickly upon the photolysis (after ~500 pulses), indicating an approximate equilibrium between the formation and decomposition.

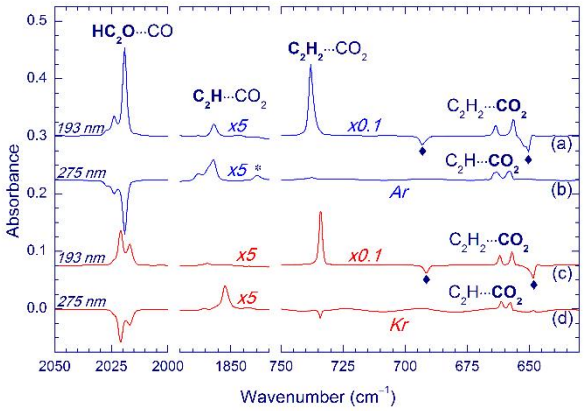

Figure 4. Formation of the $C_2H\cdots CO_2$ complex in argon (blue traces) and krypton (red traces) matrices. The difference spectra show results of (a) 193-nm photolysis of a PA/Ar (1/1000) matrix and (b) 275-nm photolysis of the same matrix. Spectra (c) and (d) show results of the same irradiations of a PA/Kr (1/1000) matrix. The bands marked by diamonds belong to PA. The band marked by an asterisk is tentatively assigned to the less stable linear (1) structure of the $C_2H\cdots CO_2$ complex. The spectra were measured at 4.3 K.

After decomposition of ~95% of PA at 193 nm (~1000 pulses), the matrix was irradiated at 275 nm (spectrum b in Fig. 4), which decomposed particularly HC_2O. Remarkably, the 1856.8 cm^{-1} band assigned to the $C_2H\cdots CO_2$ complex increased in intensity upon this irradiation and its growth correlates well with the decomposition of HC_2O (Fig. 5). The intensity of the 1856.8 cm^{-1} band increases synchronously with the intensities of the vibronic bands at higher energies as demonstrated in Fig. 5 for a vibronic band at 4069 cm^{-1}. The rising bands of CO_2 (slightly different from those of CO_2 as a monomer and in the $C_2H_2\cdots CO_2$ complex) are in a linear correlation with the C_2H bands (Fig. 5), confirming the generation of the $C_2H\cdots CO_2$ complex. The formation of the $C_2H\cdots CO_2$ complex along the decomposition of HC_2O also confirms that the latter species is complexed with CO. 275-nm light decomposes some other species in the matrix (e.g., C_3O); however, without correlation with the 1856.8 cm^{-1} band. No decomposition of $C_2H_2\cdots CO_2$ was found upon 275-nm irradiation in an argon matrix. It is important that a weak band at 1839.7 cm^{-1} (red-shifted from the band of C_2H monomer by –6.9 cm^{-1}) is visible after 275-nm photolysis in an argon matrix. It should be also noted that 275-nm light practically does not decompose PA, which explains the need of initial 193-nm photolysis.

193-nm photolysis of PA in a krypton matrix leads to products that are similar to those obtained in the argon matrix (spectrum c in Fig. 4), in agreement with the work of Isoniemi *et al.*[41] The most significant difference is the absence of bands suitable for the $C_2H\cdots CO_2$ complex in a krypton matrix. However, if 193-nm photolysis of a PA/Kr matrix is followed by irradiation at 275 nm, a characteristic band at 1852.3 cm^{-1} (blue-shifted from the band of C_2H monomer by +10.3 cm^{-1}) suitable for the $C_2H\cdots CO_2$ complex is clearly observed (spectrum d in Fig. 4). The vibronic bands of C_2H at higher energies and the CO_2 bands also rise upon 275-nm irradiation. The increase of the $C_2H\cdots CO_2$ bands linearly correlates with the decomposition of the

$HC_2O\cdots CO$ complex. The $C_2H\cdots CO_2$ bands (formed at 275 nm) are found to be efficiently bleached in a krypton matrix by 193-nm light, which is consistent with non-observation of this species after photolysis of PA at this wavelength. No bands of monomeric C_2H are observed in the experiments with photolysis of PA in both argon and krypton matrices.

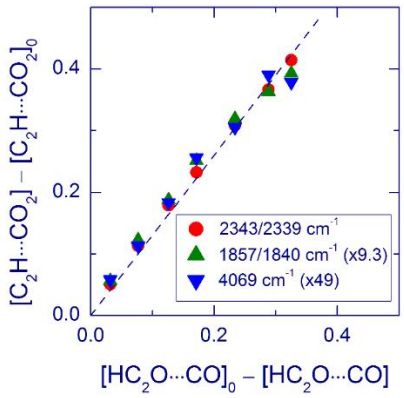

Figure 5. Correlation between the decomposition of the $HC_2O\cdots CO$ complex and the formation of the $C_2H\cdots CO_2$ complex in an Ar matrix upon irradiation at 275 nm. A PA/Ar matrix was preliminarily photolyzed at 193 nm. The vertical axis shows the increase of the relative amount of the $HC_2O\cdots CO$ complex, and the horizontal axis shows the decrease of the relative amount of the $C_2H\cdots CO_2$ complex. For the $HC_2O\cdots CO$ complex, the band at 2019.1/2023.8 cm^{-1} was integrated. The bands integrated for the $C_2H\cdots CO_2$ complex and the used multiplication factors are shown in the panel.

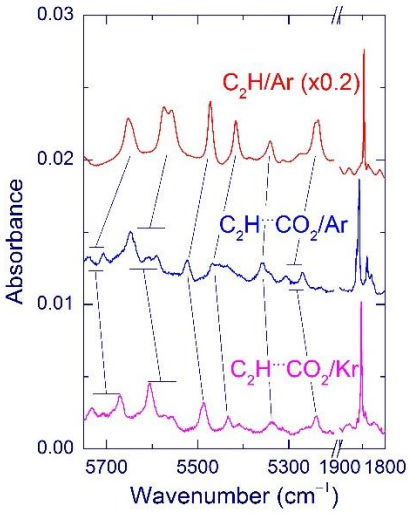

Figure 6. FTIR spectra of the $C_2H\cdots CO_2$ complex in argon and krypton matrices and of C_2H monomer in an argon matrix. The upper trace is a difference spectrum showing the result of 193-nm photolysis of a C_2H_2/Ar (1/1000) matrix. The two lower traces are difference spectra showing the result of 275-nm photolysis of a PA/Ar and PA/Kr (1/1000) matrices (after 193-nm photolysis). The spectra were measured at 4.3 K.

Fig. 6 shows the fragments of the spectra of the $C_2H\cdots CO_2$ complex in argon and krypton matrices as well as of C_2H monomer in an argon matrix. Table 3 and Table S2 (Supporting Information) present the experimental frequencies of the observed C_2H bands of the $C_2H\cdots CO_2$ complex in argon and krypton matrices, respectively. In most cases, the complexation-induced shift of the vibronic transitions of the $C_2H\cdots CO_2$ complex is larger in an argon matrix than in a krypton matrix by 10–20 cm^{-1}. Many of the $C_2H\cdots CO_2$ bands exhibit an extensive splitting (e.g., the strongest 4181/4278 cm^{-1} band in an argon matrix). In other words, the number of bands of the complex is larger than that of C_2H monomer. This splitting complicates the assignment of some bands. It should be mentioned that some bands of C_2H monomer are also structured but to a lesser extent (e.g., the 5557/5574 cm^{-1} band in an argon matrix). The relative intensities of most of the $C_2H\cdots CO_2$ bands are similar to those of C_2H monomer.

In Table 2, we compare the most characteristic frequencies and complexation-induced shifts of the $C_2H\cdots CO_2$ complex in argon and krypton matrices and the corresponding theoretical values for the parallel and linear (1) structures. As a rule, the experimental $C_2H\cdots CO_2$ bands are blue-shifted from the C_2H monomer bands (tens of cm^{-1}) in both matrices. As stated above, these blue shifts make us to conclude that the parallel structure is mainly formed in experiment. This channel is very reasonable, because the parallel structure has a bigger interaction energy than the linear (1) structure.

Finally, we describe our observations on the CO_2 absorptions of the $C_2H\cdots CO_2$ complex. These absorptions are impossible to see in the "normal" spectra because they partially overlap with the strong bands of the $C_2H_2\cdots CO_2$ complex. However, they are clearly visible in the difference spectra showing the result of 275-nm irradiation (Fig. 4 and Table 4). As mentioned above, the intensities of these bands linearly correlate with those of complexed C_2H (Fig. 5). The bending mode of complexed CO_2 is split upon the complex formation (similarly to the case of $C_2H_2\cdots CO_2$) whereas the splitting of the stretching band is probably connected with the matrix-site effect as in the case of CO_2 monomer.

Table 4. Experimental and calculated vibrational frequencies (in cm^{-1}) of CO_2 monomer and of CO_2 in the $C_2H\cdots CO_2$ complex.

Experiment (Ar)		Experiment (Kr)		Calculated shift[a]	
Mon.[b]	Compl.[c]	Mon.[b]	Compl.[c]	Par.	Lin. (1)
2345.0	2343.5	2340.5	2340.3	+0.6	+5.7
	(–1.5)	2336.6	(–0.2)		
2339.4	2339.3		2336.9		
	(–0.1)		(+0.3)		
663.5	663.3	660.5	661.4	–0.1	+0.4
662.0	(–0.2)[d]		(+0.9)		
	658.1		657.8	–9.0	
	(–5.4)[d]		(–2.7)		

[a] Calculations at the RMP2/aug-cc-pVTZ level of theory. [b] Data for CO_2 monomer from Ref. [71] [c] The experimental shifts are shown in parenthesis. [d] Calculated with respect of the more intense band of the monomer.

Concluding remarks

In the present work, we have studied the vibronic spectrum of the $C_2H\cdots CO_2$ complex, both experimentally and theoretically. In the experiments, this complex was prepared by UV photochemistry of propiolic acid (PA) in argon and krypton matrices, and the best results were obtained using two-step photolysis (193 and 275 nm). The experimental bands of C_2H in the $C_2H\cdots CO_2$ complex are blue-shifted from the corresponding bands of C_2H monomer. Practically all strong bands predicted by theory (with intensities >30 km mol^{-1}) are observed in the experiment. No bands of C_2H monomer appear in these experiments, which shows the

benefit of the preparation of the complex by photolysis of PA.

The calculations of the $C_2H\cdots CO_2$ complex structures were performed at the restricted second order Møller-Plesset (RMP2) level of theory with the aug-cc-pVTZ basis set. Four potentially stable structures were obtained in these calculations (Fig. 1); however, only two of them have a negative interaction energy after applying the higher level of theory (RCCSD(T) with the aug-cc-pVQZ basis set) and ZPVE and BSSE corrections. The *ab initio* calculation of the vibronic spectrum of the $C_2H\cdots CO_2$ complex at the same level of theory as C_2H monomer is impossible with the available computational and theoretical tools, and a simplified approach was developed. The effect of CO_2 complexation on C_2H was modeled by changing the energy of the electronic states with respect to those of C_2H monomer. The efficiency of this approach is justified by the good agreement with the experiment.

Based on these calculations, the main experimental bands of the $C_2H\cdots CO_2$ complex are assigned to the most stable parallel structure (Table 2, Table 3, and Table S2 in Supporting Information). The proposed assignment is also supported by the bands of CO_2 in the complex. Indeed, the agreement between the experimental and theoretical frequencies of the CO_2 bands is most suitable for the parallel structure (Table 4). A small admixture of the other complex structure is possible. In particular, a weak band at 1839.7 cm^{-1} observed in an argon matrix after 275-nm irradiation shows a shift of –6.9 cm^{-1} from the band of C_2H monomer, which fits well the linear (1) structure (theoretical shift of –7.1 cm^{-1}). However, no vibronic bands of this weaker complex were found.

The agreement between the experimental and theoretical results for C_2H in the $C_2H\cdots CO_2$ complex is quite good, considering the number of used approximations and the complexity of the studied system. The calculated shifts tend to be larger than the experimental ones, especially in a krypton matrix. We believe that this mismatch can be at least partially explained by the matrix effect. Indeed, the calculations are performed for the system in a vacuum whereas the experiments are made in a polarizable medium. The agreement with theory seems to be better for the less polarizable medium (argon). Prediction of matrix effects is an extremely complicated task, which exceeds the scope of the present work. The extensive splitting of some bands upon the complex formation may be caused by the matrix-site effect especially taking into account that a number of the C_2H monomer bands also have some structure.

We have no strong experimental indications that the complexation changes the intensities of the C_2H vibronic transitions, which is predicted by theory. In particular, this concerns the calculated bands of the monomer at 3604.6 and 3604.4 cm^{-1} that show a great redistribution of the intensities upon complexation. According to the calculations, the monomer absorption at 3604.4 cm^{-1} is very weak (6.9 km mol^{-1}) but the corresponding transition of the complex at 3642.8 cm^{-1} has enough intensity to be observed (152.7 km mol^{-1}). On the contrary, the monomer absorption at 3604.6 cm^{-1} is rather strong (702.7 km mol^{-1}) but the corresponding transition of the complex at 3621.7 cm^{-1} is predicted to be weak (16.6 km mol^{-1}). In the experiment, we observe a doublet for the monomer (3609/3614 cm^{-1}) and a doublet for the complex (3627/*3656* cm^{-1}) in an argon matrix; however, we cannot say whether these bands originate from the same or different transitions. The predicted enhancement of the 4209.4 cm^{-1} band upon complexation seems to agree with the appearance of a broad and intense band around 4278 cm^{-1}, in addition to the 4181 cm^{-1} band.

Our experimental observations and theoretical treatment of the observed effect are extraordinary and remarkable. The literature examples of the effects of noncovalent interactions on electronic transitions are quite limited. On the theoretical side, very few examples of calculations of excited states of complexes involving more than four atoms have been reported.[63–66] This kind of investigation is still at its infancy, mainly due to the extreme difficulty of managing the excited states at a level of accuracy as good as achieved for the ground states.[11]

On the experimental side, Kang and Pratt have reviewed the interaction of argon, nitrogen, and water with various aromatic molecules studied by high-resolution electronic spectroscopy.[67] Their review is focused on the determination of the structures, charge distributions, and internal motions of these complexes. Both red and blue shifts up to one hundred cm^{-1} were reported. A recent review by Becucci and Melandri describes other interesting examples of excited state of complexes investigated by means of high-resolution spectroscopic techniques, with emphasis on recent experiments involving anisole complexes.[68]

Experimental studies of excited electronic states of complexes involving radicals are even scarcer. Sun and Bernstein have compared the interaction of benzene and benzyl and cyclopentadienyl radicals with a nitrogen molecule.[69] They found that the origin of the first electronic transition of these molecules in the complexes could be either blue or red shifted compared to the monomers. The closest example to our system seems to be the complexes of NCO radical with Ar, N_2, CH_4, and CF_4.[70] Using the laser-induced fluorescence method, the $A^2\Pi \leftarrow X^2\Pi$ and $B^2\Sigma^+ \leftarrow X^2\Pi$ electronic transitions of NCO in the complexes were found to be blue-shifted up to 90 cm^{-1}. All of these experimental studies were performed in the UV-visible range on electronic transitions, and no theoretical explanation of the observed spectral changes was presented. In contrast, our work is made in the infrared region on vibronic transitions and we present a theoretical interpretation of the experimental observations based on *ab initio* computations.

Finally, we comment on the preparation of the $C_2H\cdots CO_2$ complex in these experiments. In both argon and krypton matrices, the $C_2H\cdots CO_2$ complex was generated by 275-nm light after 193-nm photolysis of PA. Based on the obtained correlations (Fig. 5), we suggest that this species is formed from the $HC_2O\cdots CO$ complex, probably via the C_2H + O + CO intermediate. It follows that the intuitive mechanism of the $C_2H\cdots CO_2$ complex formation involving direct photolysis of the $C_2H_2\cdots CO_2$ complex is not obvious any more. It is also possible that the $C_2H\cdots CO_2$ complex originates from decomposition of the $HC_2O\cdots CO$ complex even at 193 nm in an argon matrix. Remarkably, the $C_2H\cdots CO_2$ complex is not observed in a krypton matrix after 193-nm irradiation at all. Most probably, this complex is formed in some amounts but it is very efficiently decomposed at 193 nm. The efficient decomposition of the

$C_2H\cdots CO_2$ complex at this wavelength in a krypton matrix was directly demonstrated. Evidently, monomeric C_2H in a krypton matrix is much more stable to 193-nm light than the $C_2H\cdots CO_2$ complex; thus, the complexation of C_2H_2 with CO_2 drastically changes its UV photochemistry. The stability of the $C_2H\cdots CO_2$ complex upon 193-nm photolysis is higher in an argon matrix demonstrating an interesting solvation effect. These photochemical aspects are outside the scope of the present work.

Experimental Section

PA (≥98%, Alfa Aesar) was degassed by several freeze-pump-thaw cycles. Argon (>99.9999%, Linde) and krypton (>99.999%, Linde) were used as purchased. The gas PA/Ng (Ng = Ar and Kr) mixtures were made in a glass bulb by using standard manometric technoques. Since PA is easily adsorbed on glass surfaces, the bulb was passivated with PA vapors by several fill-keep-evacuate cycles prior to mixture preparation. The PA/Ng (1/1000) matrices were deposited onto a CsI substrate held at 15 and 20 K for argon and krypton, respectively, in a closed-cycle helium cryostat (RDK-408D2, SHI). The PA/Ng matrices were photolyzed with an excimer laser at 193 nm (MSX-250, MPB, 1 Hz, ~4 mJ cm^{-2}) and with an optical parametric oscillator at 275 nm (OPO Sunlite, Continuum, 10 Hz, ~5 mJ cm^{-2}). The IR absorption spectra in the 6300–600 cm^{-1} range were measured at 4.3 K using an FTIR spectrometer (Vertex 80, Bruker) equipped with an MCT-B detector with 1 cm^{-1} resolution and 500 scans. Reference experiments were performed with C_2H_2/Ar and C_2H_2/Kr (1/1000) matrices.

Acknowledgements

This work was supported by the Academy of Finland (projects No. 1277993 and No. 1288889). Knut Willmann is thanked for measuring the reference spectra.

Keywords: vibronic transition • noncovalent interaction • radical • quantum chemical calculations • matrix isolation infrared spectroscopy

[1] *Structure and Dynamics of Weakly Bound Molecular Complexes* (Ed.: A. Weber) Reidel: Dordrecht, **1987**.
[2] K. Müller-Dethlefs, P. Hobza, *Chem. Rev.* **2000**, *100*, 143–167.
[3] A. S. Borovik, *Acc. Chem. Res.* **2005**, *38*, 54–61.
[4] D. A. Britz, A. N. Khlobystov, *Chem. Soc. Rev.* **2006**, *35*, 637–659.
[5] J. Cerny, P. Hobza, *Phys. Chem. Chem. Phys.* **2007**, *9*, 5291–5303.
[6] D. Strmcnik, K. Kodama, D. van der Vliet, J. Greeley, V. R. Stamenkovic, N. M. Markovic, *Nature Chem.* **2009**, *1*, 466–472.
[7] E. R. Johnson, S. Keinan, P. Mori-Sanchez, J. Contreras-Garcia, A. J. Cohen, W. Yang, W. *J. Amer. Chem. Soc.* **2010**, *132*, 6498–6506.
[8] R. R. Knowles, E. N. Jacobsen, *Proc. Nat. Acad. Sci.* **2010**, *107*, 20678–20685.
[9] O. Altintas, C. Barner-Kowollik, *Macromol. Rap. Comm.* **2012**, *33*, 958–971.
[10] S. E. Wheeler, J. W. G. Bloom, *J. Phys. Chem. A* **2014**, *118*, 6133–6147.
[11] J. Řezáč, P. Hobza, *Chem. Rev.* **2016,** *116*, 5038–5071.
[12] H. Köppel, W. Domcke, L. S. Cederbaum, *Adv. Chem. Phys.* **1984,** *57*, 59–246.
[13] W. Domcke, D. R. Yarkony, *Annu. Rev. Phys. Chem.* **2012,** *63,* 325–352.
[14] M. E. Jacox, W. B. Olson, *J. Chem. Phys.* **1987,** *86,* 3134–3142.
[15] R. Tarroni, S. Carter, *J. Chem. Phys.* **2003,** *119*, 12878–12889.
[16] K. D. Tucker, M. L. Kutner, P. Thaddeus, *Astrophys. J.* **1974**, *193*, L115–L119.
[17] H. Vanlook, J. Peeters, *J. Phys. Chem.* **1995**, *99*, 16284–16289.
[18] R. Sumathi, J. Peeters, M. T. Nguyen, *Chem. Phys. Lett.* **1998**, *287*, 109–118.
[19] F. Goulay, D. L. Osborn, C. A. Taatjes, P. Zou, G. Meloni, S. R. Leone, *Phys. Chem. Chem. Phys*. **2007**, *9*, 4291–4300.
[20] W. R. M. Graham, K. I. Dismuke, W. Weltner Jr, *J. Chem. Phys.* **1974**, *60*, 3817–3823.
[21] D. P. Gilra, *J. Chem. Phys.* **1975,** *63*, 2263–2264.
[22] P. G. Carrick, A. J. Merer, R. F. Curl Jr, *J. Chem. Phys.* **1983**, *78*, 3652–3658.
[23] S. Boye, A. Campos, S. Douin, C. Fellows, D. Gauyacq, N. Shafizadeh, Ph. Halvick, M. Boggio-Pasqua, *J. Chem. Phys.* **2002,** *116*, 8843–8855.
[24] F. J. Adrian, V. A. Bowers, *Chem. Phys. Lett.* **1976**, *41*, 517–520.
[25] M. Jinguji, C. A. McDowell, *J. Mol. Struct.,* **1985**, *130,* 317–326.
[26] J. Forney, M. E. Jacox, W. E. Thompson, *J. Mol. Spectrosc.* **1995**, *170*, 178–214.
[27] G. Herzberg, *Molecular Spectra and Molecular Structure. III. Electronic Spectra and Electronic Structure of Polyatomic Molecules,* Van Nostrand, New York, 1966
[28] S. Carter, N. C. Handy, C. Puzzarini, R. Tarroni, P. Palmieri, *Mol. Phys.* **2000,** *98*, 1697–1712.
[29] R. Tarroni, S. Carter, *Mol. Phys.* **2004,** *102*, 2167–2179.
[30] D. W. Tokaryk, M. Vervloet, T.-T. Phi, *J. Mol. Spectrosc.*, **2015,** *310*, 113–118.
[31] A. T. Le, G. E. Hall, T. J. Sears, *J. Chem. Phys.* **2016,** *145,* 074306.
[32] R. Tarroni, *Chem. Phys. Lett.* **2003,** *380*, 624–631.
[33] R. Tarroni, S. Carter, *J. Chem. Phys.* **2005,** *123,* 014320.
[34] R. Tarroni, S. Carter, *Mol. Phys.* **2006,** *104,* 2821–2828.
[35] R. Tarroni, L. Khriachtchev, A. Domanskaya, M. Räsänen, E. Misochko, A. Akimov, *Chem. Phys. Lett*. **2010,** *493*, 220–224.
[36] C. Zhu, M. Räsänen, L. Khriachtchev, *J. Chem. Phys.* **2015,** *143*, 244319.
[37] C. Zhu, L. Duarte, L. Khriachtchev, *J. Chem. Phys*. **2016,** *145*, 074312.
[38] *Physics and Chemistry at Low Temperatures* (Ed.: L. Khriachtchev) Pan Stanford Publishing, Singapore, 2011.
[39] N. A. Young, *Coord. Chem. Rev.* **2013**, *257*, 956–1010.
[40] L. Khriachtchev, *J. Phys. Chem. A* **2015**, 119, 2735–2746.
[41] E. Isoniemi, L. Khriachtchev, M. Makkonen, M. Räsänen, *J. Phys. Chem. A* **2006,** *110*, 11479–11487.
[42] G. Maier, C. Lautz, *Eur. J. Org. Chem.* **1998**, 769–776.
[43] L. Khriachtchev, H. Tanskanen, A. Cohen, R. B. Gerber, J. Lundell, M. Pettersson, H. Kiljunen, M. Räsänen. *J. Am. Chem. Soc.,* **2003**, *125*, 6876–6877.
[44] H. Tanskanen, S. Johanson, A. Lignell, L. Khriachtchev, M. Räsänen, *J. Chem. Phys.* **2007**, *127*, 154313.
[45] J. Pacansky, H. Coufal, *J. Chem. Phys.* **1979**, *71*, 2811–2817.
[46] J. Pacansky, H. Coufal, *J. Chem. Phys.* **1980**, *72*, 3298–3303.
[47] J. Pacansky, D. W. Brown, J. S. Chang, *J. Phys. Chem.* **1981**, *85*, 2562–2567.
[48] J. Pacansky, D. W. Brown, *J. Phys. Chem.* **1983**, *87*, 1553–1559.
[49] Molpro, version 2010.1, a package of ab initio programs, 2010. H.-J. Werner, P.J. Knowles, F.R. Manby, M. Schütz, P. Celani, G. Knizia, T. Korona, R. Lindh, A. Mitrushenkov, G. Rauhut, T. B. Adler, R. D. Amos, A. Bernhardsson, A. Berning, D. L. Cooper, M. J. O. Deegan, A. J. Dobbyn, F. Eckert, E. Goll, C. Hampel, A. Hesselmann, G. Hetzer, T. Hrenar, G. Jansen, C. Köppl, Y.Liu, A. W. Lloyd, R. A. Mata, A. J. May, S. J. McNicholas, W. Meyer, M. E. Mura, A. Nicklass, P. Palmieri, K. Pflüger, R. Pitzer, M. Reiher, T. Shiozaki, H. Stoll, A. J. Stone, R. Tarroni, T. Thorsteinsson, M. Wang, A. Wolf. See http://www.molpro.net.
[50] R. D. Amos, J. S. Andrews, N. C. Handy, P. J. Knowles, *Chem. Phys. Lett.* **1991,** *185*, 256–264.

[51] D. J. Tozer, N. C. Handy, R. D. Amos, J. A. Pople, R. H. Nobes, Y. Xie, H. F. Schaefer, *Mol. Phys*. **1993,** *79*, 777–793.
[52] T. H. Dunning, Jr. *J. Chem. Phys*. **1989,** *90,* 1007–1023.
[53] R. A. Kendall, T. H. Dunning, Jr., R. J. Harrison, *J. Chem. Phys.* **1992,** *96*, 6796–6806.
[54] P. J. Knowles, C. Hampel, H.-J. Werner, *J. Chem. Phys*. **1993,** *99*, 5219–5227.
[55] J. D. Watts, J. Gauss, R. J. Bartlett, *J. Chem. Phys.* **1993,** *98,* 8718–8733.
[56] S. F. Boys, F. Bernardi, *Mol. Phys.* **1970,** *19*, 553–566.
[57] C. Lauzin, K. Didriche, J. Lievin, M. Herman, A. Perrin, *J. Chem. Phys*. **2009**, *130*, 204306.
[58] G. Donoghue, X.-G. Wang, R. Dawes, T. Carrington, Jr., *J. Mol. Spectrosc.* **2016**, *330,* 170–178.
[59] M. E. Jacox, *J. Phys. Chem. Ref. Data* **2003,** *32*, 1–441.
[60] E. F. C. Byrd, C. D. Sherrill, M. Head-Gordon, *J. Phys. Chem*. *A* **2001,** *105*, 9736–9747.
[61] H. J. Werner, P. J. Knowles, *J. Chem. Phys*. **1988**, *89*, 5803–5814.
[62] R. J. Bartlett, M. Musiał, *Rev. Mod. Phys.* **2007,** *79*, 291–352.
[63] V. Barone, M. Biczysko, M. Pavone, *Chem. Phys.* **2008,** *346,* 247–256.
[64] J. L. C. Fajín, S. B. Capelo, B. Fernandez, P. M. Felker, *J. Phys. Chem. A* **2007,** *111*, 7876–7881.
[65] H. Koch, B. Fernandez, O. Christiansen, *J. Chem. Phys.* **1998,** *108*, 2784–2790.
[66] G. Pietraperzia, M. Pasquini, F. Mazzoni, G. Piani, M. Becucci, M. Biczysko, D. Michalski, J. Bloino, V. Barone, *J. Phys. Chem. A* **2011,** *115*, 9603–9611.
[67] C. Kang, D. W. Pratt, *Int. Rev. Phys. Chem.* **2005,** *24*, 1–36.
[68] M. Becucci, S. Melandri, *Chem. Rev.* **2016,** *116*, 5014–5037.
[69] S. Sun, E. R. Bernstein, *J. Chem. Phys*., **1995,** *103*, 4447–4454.
[70] J. Yao, J. A. Fernandez, E. R. Bernstein, *J. Chem. Phys*. **1997,** *107,* 8813–8822.
[71] S. V. Ryazantsev, V. I. Feldman, *J. Phys. Chem. A* **2015**, *119*, 2578–2586.

Here is the first study of the effect of noncovalent interaction on vibronic transitions and the first report on an intermolecular complex of C_2H radical. The $C_2H\cdots CO_2$ complex was prepared by UV photochemistry of propiolic acid (HC_3OOH) in argon and krypton matrices. In order to simulate the infrared spectrum of the $C_2H\cdots CO_2$ complex, we developed the theoretical approach used earlier for C_2H monomer.

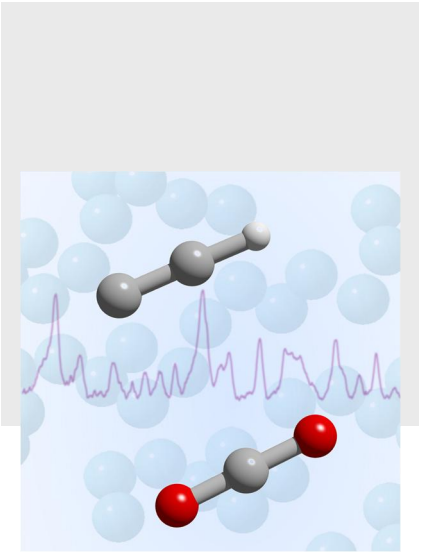

*Sergey V. Ryazantsev, Riccardo Tarroni, Vladimir I. Feldman, and Leonid Khriachtchev**

Page No. – Page No.

Effect of noncovalent interactions on vibronic transitions: An experimental and theoretical study of the $C_2H\cdots CO_2$ complex